Available online at www.sciencedirect.com
SCIENCE DIRECT®
International Journal of Heat and Fluid Flow 25 (2004) 159–172
International Journal of HEAT AND FLUID FLOW
www.elsevier.com/locate/ijhff

Experimental evaluation of flow boiling incipience of subcooled fluid in a narrow channel

Magdalena Piasecka, Sylwia Hozejowska, Mieczyslaw E. Poniewski *

Chair of Thermodynamics and Fluid Mechanics, Kielce University of Technology, Al. 1000-lecia P.P. 7, Kielce PL 25-314, Poland

Abstract

Experimental investigations dealt with heat transfer of R123 flowing through a narrow vertical channel of 1 mm height with one wall heated uniformly and others approximately adiabatic. Particular attention was paid to boiling incipience conditions and nucleate hysteresis phenomena. An inverse problem was dealt with as, on the basis of temperature measurement on external side of the heating foil (with thermography technique) and the measurement of the electric power supplied to this foil, it was possible to determine local heat transfer coefficients on the contact surface of the heating wall and the fluid flowing along the narrow channel. Two models of heat transfer through the heating foil and the isolating glass into the boiling liquid were proposed and discussed: one- and two-dimensional. In order to solve the two-dimensional inverse heat conduction problem the method of thermal polynomials was used with application of the least square and Trefftz computational techniques. Some exemplary results of numerical calculations on the basis of experimental data were presented for both models. The correlations concerning Nusselt number determination for R123 boiling incipience in vertical narrow channel were developed.

1. Introduction

An increasing number of high-tech heat exchange devices are based on heat transfer to liquids during flow boiling in narrow channels of various geometry and orientation. Owing to the change of state, which accompanies boiling, it is possible to simultaneously meet contradictory demands, i.e. to obtain the heat flux as large as possible at small temperature difference between the heating surface and the saturated liquid and, at the same time, keep small dimensions of heat transfer systems. On the other hand, boiling incipience, the appearance of the first bubbles, is not only a fundamental problem in boiling heat transfer but also a practical one in the evaluation of the safety of equipment such as for example, electronic devices or nuclear reactors. It is known, that under some circumstances, there can occur a considerable wall temperature rise above the liquid saturation temperature before boiling begins. Under some conditions, the temperature level required to initiate boiling may be larger than the allowable maximum wall temperature of the system. It could result in the destruction of the object being cooled, already in the single-phase regime. This ''temperature overshoot'' called ''nucleate hysteresis'', ''zero boiling crisis'', ''superheated excursion'' is significant when highly wetting dielectric fluids are used. Thus heat transfer coefficient and heat flux accompanying the incipience of nucleate boiling in narrow channels and its behaviour under some conditions constitute some of the most important issues of heat transfer mechanism. Relying on the knowledge of boiling incipience, we can guarantee safe operation of devices.

The authors' main goals were experimental and theoretical investigations into boiling incipience in a rectangular vertical narrow channel, where an external wall was heated uniformly and others were assumed to be quasiadiabatic. The authors wanted to determine the impact of various factors, namely pressure, the inlet liquid subcooling and the flow velocity on boiling incipience. Another task was to analyse boiling curves obtained in the experiment.

* Corresponding author. Tel.: +48-41-3424334; fax: +48-41-3424340.
E-mail address: tmpmp@tu.kielce.pl (M.E. Poniewski).

0142-727X/$ - see front matter © 2003 Elsevier Inc. All rights reserved.
doi:10.1016/j.ijheatfluidflow.2003.11.017

Nomenclature

A	cross-section, m^2
c_{pl}	specific heat of liquid, J/kg K
c, d	coefficients
D	diameter, m
G	liquid mass velocity, kg/m^2 s
h_{lv}	latent heat of vaporisation, J/kg
H	height, m
I	current supplied to the heating foil, A
i, j, n	natural numbers (i - square root of 1)
L	length, m
M, N	total number of heat polynomials
O	perimeter, m
p	pressure, N/m^2
Q_V	volumetric flow rate, m^3/s
q	heat flux density, W/m^2
q_V	capacity of internal heat source, W/m^3
T	temperature, K
u	liquid velocity, m/s
u_n	harmonic polynomials
W	width, m
X, Y, Z	axes of Cartesian coordinate system
x, y	locations (x—distance from the channel inlet), m

Greeks

$\alpha(x)$	local heat transfer coefficient, W/m^2 K
$\alpha_1(x)$	local heat transfer coefficient, obtained from one-dimensional model, W/m^2 K
$\alpha_2(x)$, $\alpha_2'(x)$	local heat transfer coefficient, obtained from two-dimensional model with application of: (1) the least square method and (2) the Treffz method, W/m^2 K
δ	width, m; standard error
ΔT_{sat}	surface superheating, $T_w - T_{sat}$, K
ΔT_{sub}	inlet liquid subcooling $(T_{sat} - T_l)_{inlet}$, K
ΔU	the voltage drop across the foil, V
θ	approximate temperature
λ	thermal conductivity, W/m K
μ	dynamic viscosity, kg/ms
ρ	density, kg/m^3
σ	surface tension, N/m

Subscripts

BI	boiling incipience
ch	narrow channel
F	foil
G	glass
h	hydraulic
he	heated
l	liquid/mixture of liquid and vapour
sat	saturation
w	wall

2. Brief review of literature

There are not many works published on heat transfer experimental investigations and theoretical analysis for various liquids (distilled water, methanol) flow boiling through rectangular vertical uniformly heated narrow channels of various dimensions. We could mention here Peng and Wang (1993, 1994); Peng et al. (1995, 1996, 1998, 2000, 2001a,b); Peng and Peterson (1995, 1996); Wang and Peng (1993, 1994). The authors were interested, among others, in the impact of different parameters (channel geometry, liquid subcooling, flow velocity) on flow boiling in narrow channels. They also looked into the flow patterns in narrow channel boiling.

Orozco and Hanson (1992) investigated boiling in asymmetrically heated narrow channels of various depths, inclined at different angles to the horizon. The researchers focused on the impact of selected parameters (different geometry of narrow channels, spatial orientation, liquid temperature at the inlet, flow velocity) on R113 flow boiling.

Chin (1997) and Chin et al. (1998a,b) dealt with heat transfer in R11 flow through vertical narrow channel heated asymmetrically. The set-up Chin constructed was similar to that one shown in the present paper. The experiments were carried out in the area of forced convection, boiling incipience and developed nucleate boiling; in laminar and turbulent flows.

In the experiments of Bao and others, (Bao et al., 2000a,b), R11 and HCFC 123 flowed through a uniformly heated, horizontally located narrow conduit. The local heat transfer coefficient in the boiling zone was investigated. The impact of selected factors (mass flux, heat flux density, vapour quality and the system pressure) was examined.

Yan and Lin (1998) gave the results of their experiments which aimed at determining heat transfer coefficient and pressure drop while R134a flowed through 28 small circular pipes, which constituted a symmetrically heated plane bundle.

Ammerman and You (1998) used FC-87, which flowed through asymmetrically heated horizontal narrow channel of different square cross-sections. They were interested in heat transfer in boiling and forced convection. It was found that the channel dimensions decrease enhances heat transfer and is advantageous to the occurrence of higher heat transfer coefficients.

Wambsganss et al. (1993) conducted experiments on heat transfer with R113 flowing through a symmetrically

heated circular narrow channel. The results of heat transfer coefficients were compared with those calculated on the basis of correlations proposed by other authors. Wambsganss and others also identified the flow patterns, which occurred in flow boiling in narrow channels, both circular and rectangular (Wambsganss et al., 1991, 1993).

Kuznetsov and Shamirzaev (1999) presented the results of experiments for R318C flow through a horizontal annular narrow channel. Heat transfer coefficient values were determined for various flow patterns and compared with those calculated from well-known correlations.

Heat transfer experiments under the conditions of forced convection were of interest for Adams et al. (1998, 1999a,b). In those experiments the agent flowed, in a turbulent manner, through uniformly heated narrow channels of different hydraulic diameter located horizontally and vertically. The agent was distilled water or water-dissolved air mixture. The Nusselt number determined experimentally was compared with the values obtained with known correlations.

Ghiaasiaan and Laker (2001) relied on Adams's results (Adams et al., 1998, 1999a,b) to conduct heat transfer analysis of water turbulent flow through circular narrow channels. The authors wanted to explain irregularities and contradictory data concerning heat transfer coefficient and friction factor.

Lazarek and Black (1992) conducted experiments into boiling heat transfer while R113 flowed through a vertical circular narrow channel. The authors presented their equation for Nusselt number. They also observed the phenomenon of "nucleation hysteresis" occurring in the flow through minichannels, similarly to Chin (1997), Chin et al. (1998a,b), Orozco and Hanson (1992) and Simon (1991). There are only a few surveys providing experimental results, which aim at finding a theoretical explanation of boiling incipience and accompanying "nucleation hysteresis" (Turton, 1968; Brauer and Mayinger, 1992; Bar-Cohen, 1992; Celata et al., 1992; Poniewski et al., 2000).

The fact that there are not many works on heat transfer in boiling and forced convection in narrow channels results from the amount of difficulties the experiments involve. Boiling curves and local heat transfer coefficients, which come as the result of experimental investigations and theoretical analysis, including correlations, demonstrate high scatter. The measurements were taken for a rather small range of variability of parameters such as flow rate, pressure and the liquid subcooling. Boiling incipience and accompanying it nucleation hysteresis during subcooled refrigerant flow through a narrow channel seem a good choice as the subject matter of the experimental and theoretical research. Such investigations are important for practical engineering applications.

3. Experimental stand and procedure

The diagram of the main loop of the flowing system is shown in Fig. 1. It consists of: test section with a vertical narrow channel, rotary pump, compensating tank, heat exchangers, rotameters and pressure converters.

The diagram of the test section is presented in Fig. 2. A narrow channel of 1 mm height, 40 mm width, 360 mm length was built in the test section basic part. The heating element for working fluid (R123), which flows along the narrow channel from inlet conduit to outlet chamber, is an alloy foil stretched between the front cover and the channel body. The heating element 0.004'' ($\approx$0.1 mm) foil designated as Haynes-230, made of Ni–Cr–W–Mo high-temperature alloy was selected. It is possible to observe changes in the foil surface temperature through the opening covered with the glass. There are a base coat and liquid crystals spread between the foil and the glass. Due to thermography (Piasecka, 2002; Hay and Hollingsworth, 1998) and the data acquisition system (Fig. 4), it is possible to measure temperature distribution on the heating wall. The test section rear cover contains channels, to which water is fed, or which are air gaps, Fig. 2. Due to these auxiliary channels it is possible to maintain the desirable temperature on the wall, which is treated as quasiadiabatic. There are five thermocouples soldered to the bottom wall of the water channel and two others located of the auxiliary channel inlet and outlet, Fig. 2. The narrow channel inlet and outlet is equipped with two thermocouples and two pressure converters.

Temperature distribution recording on the surface under examination is performed by the following system:

- The test section with a narrow channel (Fig. 2), where the heating foil, base coat and thermochromic liquid crystals are located, Fig. 3.
- CCD colour video camera equipped with the device decomposing video signal into the RGB signal and zoom lens with manual control located straight in front of the examined object (Figs. 3 and 4a).
- Illumination system, which consists of two white light sources located at the same distance and at the same angle with respect to the object examined. Those are

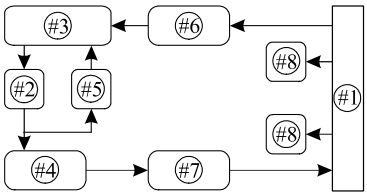

Fig. 1. The diagram of main loop of the flowing system: #1—test section with a narrow channel; #2—pump; #3—compensating tank; #4, #5, #6—heat exchangers; #7—rotameters; #8—pressure converters.

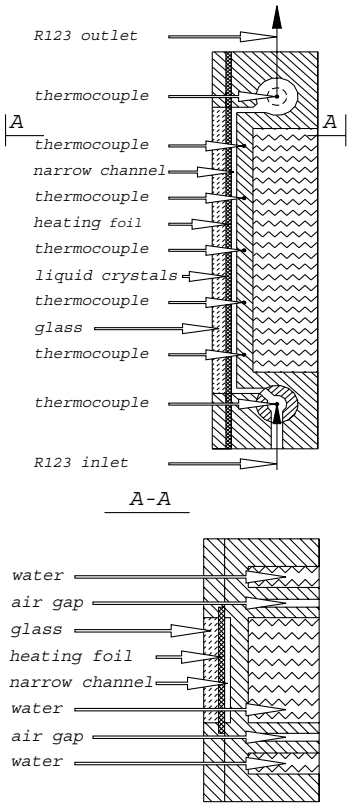

Fig. 2. Diagram of the test section.

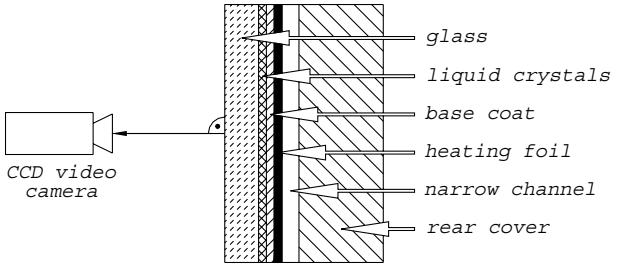

Fig. 3. The diagram of the system camera—test section.

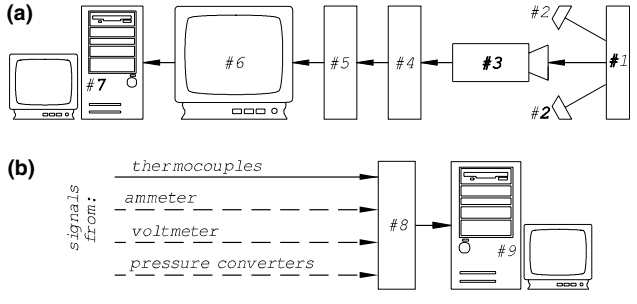

Fig. 4. The diagram of the system of acquisition of measurement data, colour images and their further processing: #1—test section; #2—lighting system; #3—video camera; #4—signal decomposer; #5—*Betacam* video recorder; #6—monitor; #7—computer with frame grabber and monitor; #8—data acquisition station; #9—computer with monitor.

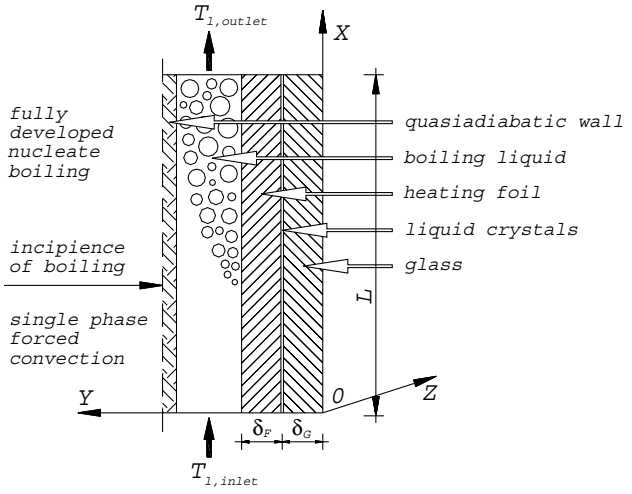

Fig. 5. One- and two-dimensional models diagram.

fluorescent lamps emitting "cool white light" (the lamps distance from the illuminated surface and the angle at which the light falls are adjustable), Fig. 4a.

The diagram of the system of acquisition of colour images and their further processing is presented in Fig. 4a. The system allows colour image projection directly on the computer monitor in real time, image preservation in RGB format and its transfer to the computer for further analysis, simultaneous projection of the real time image on the recorder monitor as well as the image recording on the video tape. The software working with frame grabber and the one processing the measurement data complements the system. The registration of the remaining measurement data is carried out with *Keithley 500 A* data acquisition station equipped with *ViewDac* software installed at another computer (Fig. 4b).

What is sought is the heat transfer coefficient during the incipience of boiling on the surface separating the heating foil and the boiling fluid (Fig. 5). That is an inverse problem, in which with application of temperature measurement at the system internal points (temperature distribution on the heating foil on the side of the glass) and the measurement of the electric power supplied to the heater, one can calculate the requested local heat transfer coefficients on the heating wall surface contacting the boiling fluid (Piasecka, 2002; Piasecka et al., 2003).

4. Experimental parameters

4.1. Quantities set

- Heat source capacity (heat flux volumetric density) q_V supplied to the heating wall, determined from the formula:

$$q_V = \frac{I \cdot \Delta U}{A_F \cdot \delta_F} \quad (1)$$

4.2. Quantities measured

Thermal and flow parameters:

- local temperature of the heating foil $T_w(x)$, determined from the hue distribution on the surface;
- the temperature of the investigated fluid at the channel inlet $T_{l,inlet}$ and outlet $T_{l,outlet}$;
- the temperature of the quasiadiabatic back wall of the narrow channel at five different points and the temperature of water at the auxiliary channel inlet and outlet;
- volumetric rate of flow Q_V, (rotameters readings);
- positive gauge pressure at the inlet p_{inlet} and outlet of the narrow channel p_{outlet} (pressure converters readings);

Electrical parameters:

- the voltage drop over a definite heating foil length ΔU;
- the current supplied to the heating foil I.

4.3. Quantities calculated

Quantities, which characterise heat transfer and the fluid flow:

- local heat flux density $q_w(x)$ and local heat transfer coefficient $\alpha(x)$, determined with the use of one- and two-dimensional models of heat transfer through the foil and glass,
- the temperature of the fluid in the narrow channel, determined form the enthalpy balance (Chin, 1997; Chin et al., 1998a,b; Piasecka, 2002):

$$T_l(x) = T_{l,inlet} + 4 \cdot \frac{q_w(x)}{G \cdot c_{pl} \cdot D_{he}} \cdot x \quad (2)$$

where D_{he}—equivalent heated diameter, $D_{he} = 4 \cdot A_{ch}/O_{he}$, O_{he}—heated perimeter, $O_{he} = H_{ch}$.

- Local Nusselt number $Nu(x)$:

$$Nu(x) = \frac{\alpha(x) \cdot D_h}{\lambda_l} \quad (3)$$

where D_h—hydraulic diameter calculated from the formula:

$$D_h = \frac{2 \cdot A_{ch}}{W_{ch} + H_{ch}} \quad (4)$$

- local surface superheating $\Delta T_{sat}(x)$:

$$\Delta T_{sat}(x) = T_w(x) - T_{sat}(x) \quad (5)$$

- subcooling at the inlet ΔT_{sub}:

$$\Delta T_{sub} = (T_{sat} - T_l)_{inlet} \quad (6)$$

- liquid flow velocity in the channel u:

$$u = \frac{Q_V}{A_{ch}} \quad (7)$$

- mass flow velocity G:

$$G = \rho_l \cdot u \quad (8)$$

- Reynolds number:

$$Re = \frac{G \cdot D_h}{\mu_l} \quad (9)$$

- local pressure in the narrow channel $p(x)$ assumed to change linearly from the channel inlet to the outlet.

The basic physical properties of the liquid are assumed in accordance with the literature (McLinden, 1995).

4.4. The range of experimental parameters

The variation range of parameters characterising experimental investigations are presented in Table 1.

4.5. Experimental procedure

On the basis of results obtained in the form of images of colour distribution on the heating foil, Fig. 6, the procedure for the experiment will be discussed. These images correspond to the temperature distribution on the heating foil, while increasing and later decreasing the heating power supplied to it.

The experiment starts with increasing the current supplied to the heating foil, during R123 laminar flow through a narrow channel. First, the heat transfer between the heating foil and the working fluid in the narrow channel proceeds by means of single phase forced convection (Fig. 6—first eight images). It is recognisable as the appearance of subsequent hues in the visible spectrum sequence and points to the gradual increase in the heating temperature surface (black colour on the surface being observed, indicates that the surface temperature is higher or lower than the liquid crystals sensitivity range). The condition, which must be met for the

Table 1
The variation range of basic parameters in experimental investigations (Piasecka, 2002)

Quantities set	q_V	[kW/m^3]	$6.63\times10^4 - 1.17\times10^6$
Quantities measured	Q_V	[m^3/s]	$3.88\times10^{-6} - 1.90\times10^{-5}$
	p_{inlet}	[kPa]	126–345
Quantities calculated	q_w	[kW/m^2]	6.7–118.8
	ΔT_{sub}	[K]	23.3–71.1
	u	[m/s]	0.10–0.48
	G	[kg/m^2 s]	143–710
	Re	[–]	618–2890

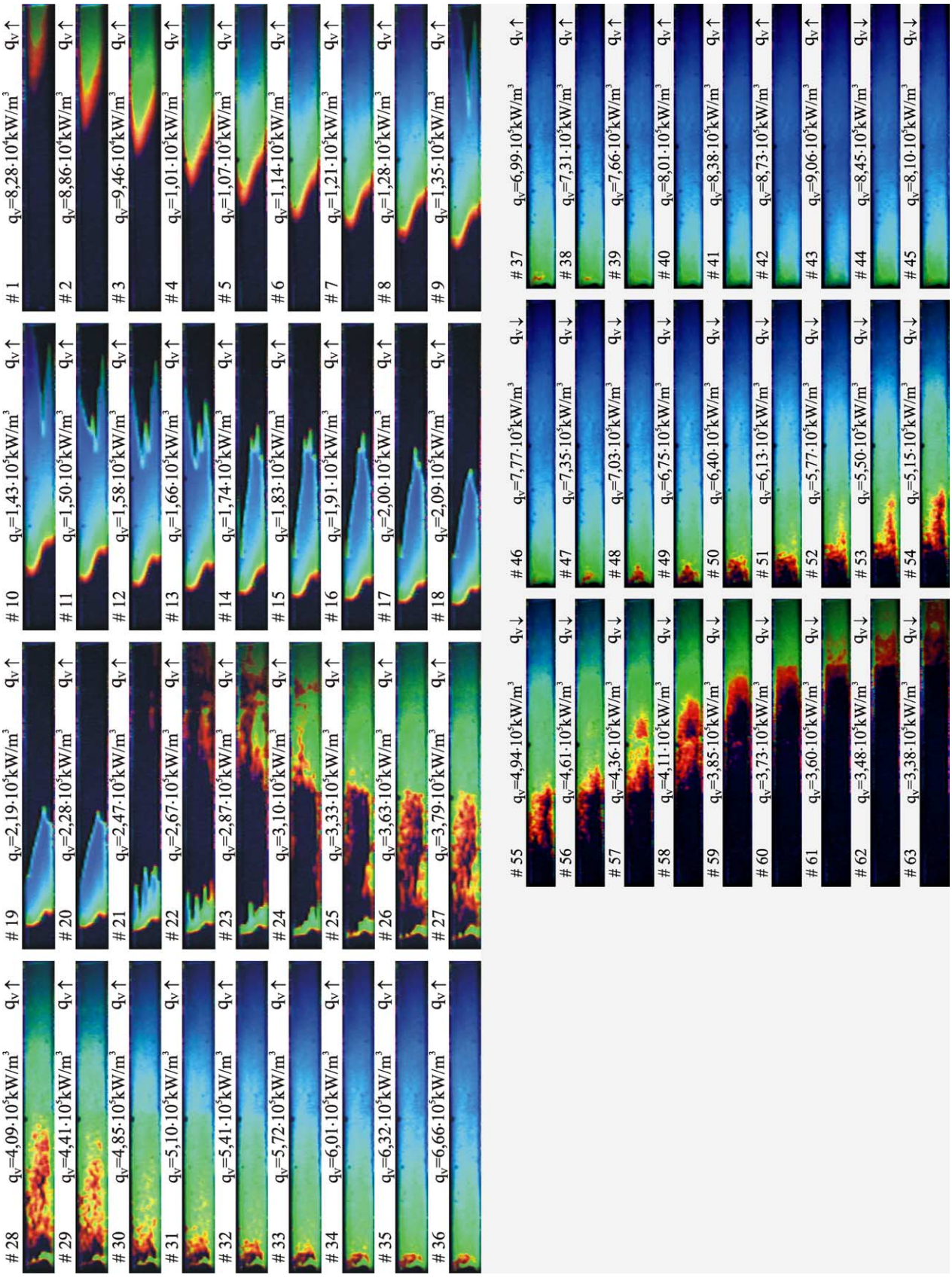

Fig. 6. Images of temperature distribution on the heating wall, $Q_V = 1.4 \times 10^{-5}$ m^3/s; $G = 524$ kg/m^2 s; $u = 0.35$ m/s; $Re = 2100$; $p_{inlet} = 180$ kPa; $\Delta T_{sub} = 33.0$ K; $q_V = 8.28 \times 10^4$–9.06×10^5 kW/m^3; $q_w = 8.4$–92.0 kW/m^2; the pre-set value q_V is given in the figure.

measurement series to begin, is the occurrence of stable "boiling front" on the heating wall (Fig. 6, image #9). It seen as vehement hue changes on the heating foil, taking place inversely to the spectrum sequence, then black hue returns. That indicates a sudden heating wall temperature drop at almost constant heat flux. It is treated as the evidence of boiling incipience (BI) and it clearly separates the region of single phase forced convection from the region where nucleate boiling occurs. When the heat flux supplied to the foil increases, the "boiling front" moves in the direction opposite to the direction of the liquid flow in the channel. It can be observed clearly while analysing images from #9 up to #27, Fig. 6. When we continue increasing the heat flux, and the heating wall temperature exceeds the sensitive range of liquid crystals, another hue change is observed on the heating surface in the visible spectrum sequence (Fig. 6, image #22). It is accompanied by pressure increase in the channel, flow fluctuations, sharp increase in the liquid temperature in the flow core and flow resistance fluctuations. All these suggest that the amount of vapour phase in the boiling vapour–liquid mixture has grown and developed nucleate boiling appeared (Fig. 6, images from #22 up to #43).

Then the current supplied to the foil is gradually reduced following the occurrence of saturated navy blue hue on the foil surface (Fig. 6, images from #44 up to #63). Mild hue changes, in the direction opposite to the spectrum sequence are observed to accompany the decrease in the current supplied to the foil. As a result, heat transfer returns to forced single phase convection. The heat flux decrease makes the boiling "fading away" start earliest at the channel front part.

5. Assumptions for both models

- The liquid crystal layer on the heating foil is very thin, therefore it is disregarded in considerations.
- In the system under investigation, the state is steady.
- Changes in the temperature of the foil and the liquid as well as the fluid velocity along the axis Z are disregarded, Fig. 5.

6. One-dimensional model

One-dimensional model put forward in (Chin, 1997; Chin et al., 1998a,b) and modified in (Piasecka, 2002; Piasecka et al., 2003) is based on the equations of energy balance for individual control volumes of the test section. The analysis was carried out in respect of isolated volumes, separately for the foil and the glass. The investigations took into account the dimension along the flow direction—X, but the dimension perpendicular to it—Y, was related only to the foil or glass thickness.

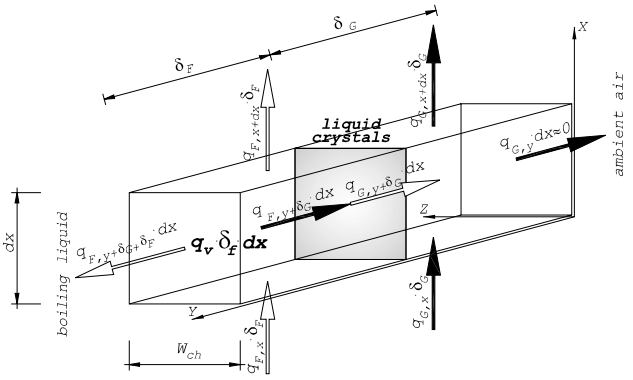

Fig. 7. The detailed energy balance in one-dimensional model.

Fig. 7 presents heat fluxes transferred to control volume of foil or glass, per narrow channel width, as the product of heat fluxes density and either the thickness or the elementary length of each layer.

The heat balance equation for control volumes can be presented as follows:

(1) for foil:

$$q_{\mathrm{F},x}\cdot\delta_{\mathrm{F}}+q_{\mathrm{V}}\cdot\delta_{\mathrm{F}}\cdot\mathrm{d}x=q_{\mathrm{F},x+\mathrm{d}x}\cdot\delta_{\mathrm{F}}+q_{\mathrm{F},y+\delta_{\mathrm{G}}}\cdot\mathrm{d}x+q_{\mathrm{F},y+\delta_{\mathrm{G}}+\delta_{\mathrm{F}}}\cdot\mathrm{d}x \tag{10}$$

(2) for glass:

$$q_{\mathrm{G},x}\cdot\delta_{\mathrm{G}}+q_{\mathrm{G},y+\delta_{\mathrm{G}}}\cdot\mathrm{d}x=q_{\mathrm{G},x+\mathrm{d}x}\cdot\delta_{\mathrm{G}} \tag{11}$$

(3) for the foil–glass interface:

$$q_{\mathrm{F},y+\delta_{\mathrm{G}}}\cdot\mathrm{d}x=q_{\mathrm{G},y+\delta_{\mathrm{G}}}\cdot\mathrm{d}x \tag{12}$$

We assume:

$$\frac{\mathrm{d}^2T_{\mathrm{F}}}{\mathrm{d}x^2}=\frac{\mathrm{d}^2T_{\mathrm{G}}}{\mathrm{d}x^2} \tag{13}$$

which constitutes the extension of the condition, which results from Eq. (12). It can be applied owing to the small thickness of the partition, in which conduction process is accounted for. At the same time, it was assumed that the derivative of the temperature gradient on the heating foil is equal to the temperature gradient on the foil surface, read from liquid crystals hue distribution.

As a result of transformations and after the introduction of the dependences resulting from Fourier's law, we obtained the local heat transfer coefficient calculated from the equation:

$$\alpha_1(x)=\frac{(\lambda_{\mathrm{F}}\cdot\delta_{\mathrm{F}}+\lambda_{\mathrm{G}}\cdot\delta_{\mathrm{G}})\cdot\left(-\frac{\mathrm{d}^2T_{\mathrm{F}}}{\mathrm{d}x^2}\right)+q_{\mathrm{V}}\cdot\delta_{\mathrm{F}}}{T_{\mathrm{F}}(x)-T_{\mathrm{l}}(x)} \tag{14}$$

In Eq. (14) it is necessary to determine the second derivative of the heating wall temperature along the narrow channel length. The method of the least squares

was applied to the function $T_F = T_F(x)$ polynomial approximation.

7. Two-dimensional model

In the two-dimensional model the dimension perpendicular to the flow direction was also taken into account (Piasecka, 2002; Piasecka et al., 2003; Hozejowski et al., 2003).

The process of heat transfer in a two-layer wall, shown in Fig. 5, is described with the following equations:

(1) in foil:

$$\frac{\partial^2 T_F}{\partial x^2} + \frac{\partial^2 T_F}{\partial y^2} = -\frac{q_V}{\lambda_F} \tag{15}$$

(2) in glass:

$$\frac{\partial^2 T_G}{\partial x^2} + \frac{\partial^2 T_G}{\partial y^2} = 0 \tag{16}$$

and the boundary conditions concerning T_G and T_F are shown in Fig. 8.

We shall use harmonic polynomials in the solution of the problem under consideration. Harmonic polynomials $u_n(x,y)$ which satisfy Eq. (15) are defined as the real and imaginary part of the holomorphic function $(x+\mathrm{i}y)^n$:

$$u_n(x,y) = \begin{cases} \mathrm{Re}\left((x+\mathrm{i}y)^{\frac{n}{2}}\right) & \text{for odd } n \\ \mathrm{Im}\left((x+\mathrm{i}y)^{\frac{n+1}{2}}\right) & \text{for even } n \end{cases} \tag{17}$$

The unknown T_G and T_F will be approximated with a linear combination of the harmonic polynomials $u_n(x,y)$:

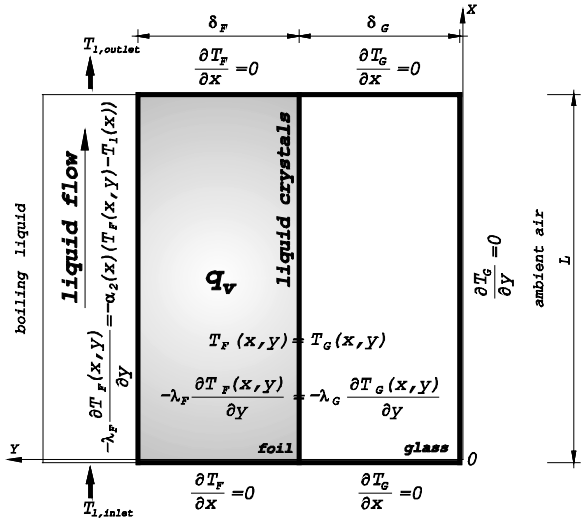

Fig. 8. Boundary conditions for a two-layer wall.

$$T_G(x,y) \approx \theta_G(x,y) = \sum_{i=0}^{N} c_i u_i(x,y) \tag{18}$$

$$T_F(x,y) - \tilde{u}(x,y) \approx \theta_F(x,y) = \sum_{j=0}^{M} d_j u_j(x,y) \tag{19}$$

where $\tilde{u}(x,y) = -\frac{q_V}{2\lambda_F} y^2$ is a particular solution of Eq. (15).

The unknown coefficients c_i $(i = 0,1,\ldots,N)$ and d_j $(j = 0,1,\ldots,M)$ are obtained with Trefftz or the least square techniques. In the computational procedure the approximation of T_G will be obtained first and T_F next. Provided $T_F(x,y)$ on the boundary $y = \delta_G + \delta_F$ is known, we are able to compute the heat transfer coefficient from the following boundary condition:

$$-\lambda_F \frac{\partial T_F(x, \delta_G + \delta_F)}{\partial y} = \alpha_2 (T_F(x, \delta_G + \delta_F) - T_l(x)) \tag{20}$$

8. Experimental results

8.1. Boiling curves

Boiling curves are obtained on the basis of data, while increasing and later decreasing the heat flux supplied to the heating foil. They are usually constructed for the selected points in the channel (at selected distance from the inlet), where heat flux density depends on the heating surface superheating $\Delta T_{sat} = T_w - T_{sat}$ at some specified points in the channel.

Boiling incipience zone is very sensitive to even slight changes in the heat flux density and pressure fluctuations. While conducting experimental observations of boiling incipience and nucleation hysteresis it is, therefore necessary to control, very accurately, all changes in the heat flux provided. The minimum and the maximum values of the heat flux supplied to the foil are limited by the sensitivity range of liquid crystals, applied to the heating surface temperature detection. The value of the temperature drop following the boiling incipience does not have to be observable in the experiment, when the heating surface temperature diminishes to the value below the liquid crystals sensitivity range, Fig. 9.

Fig. 9 shows a typical shape of a boiling curve. While increasing the heat flux density (from point **A** to point **BI**—nucleate boiling incipience), the heat transfer between the heating foil and subcooled liquid flowing upward the narrow channel proceeds by means of single phase forced convection. In the foil adjacent area, the liquid becomes superheated, point **BI**, whereas in the flow core it remains subcooled. The increase in the heat flux density results in vapour nuclei activation on the channel heating surface. Boiling incipience comes spontaneously for the superheating $\Delta T_{sat} = 25$–30 K

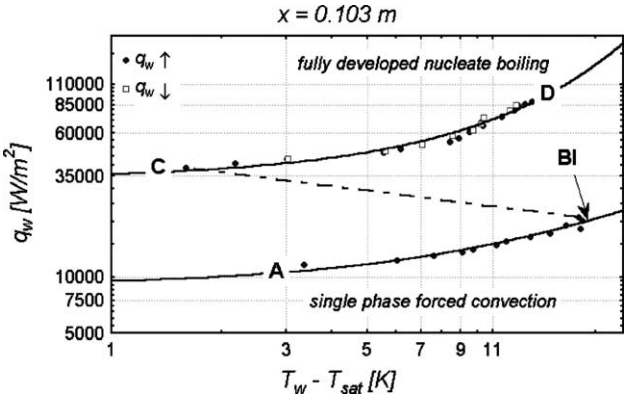

Fig. 9. Typical boiling curve, $Q_V = 1.1 \times 10^{-5}$ m^3/s; $G = 412$ kg/m^2 s; $u = 0.28$ m/s; $Re = 1\ 646$; $p_{inlet} = 190$ kPa; $\Delta T_{sub} = 36.0$ K; $q_V = 8.07 \times 10^4$–8.73×10^5 kW/m^3; $q_w = 8.2$–88.6 kW/m^2.

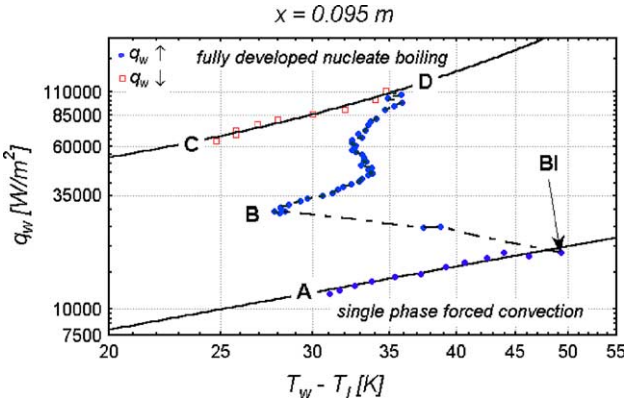

Fig. 11. Exemplary boiling curves with II kind hysteresis: $Q_V = 1.34 \times 10^{-5}$ m^3/s; $G = 501$ kg/m^2 s; $u = 0.34$ m/s; $Re = 2\ 015$; $p_{inlet} = 247$ kPa; $\Delta T_{sub} = 41.3$ K; $q_V = 1.17 \times 10^5$–8.01×10^5 kW/m^3; $q_w = 11.9$–81.4 kW/m^2.

(Piasecka, 2002), point **BI**. Spontaneous nucleation causes the heating surface temperature drop, for almost constant heat flux density. It is visible as drop from point **BI** to point **C**. Further increase in the heat flux density leads to developed nucleate boiling, section **C**–0**D**. Decreasing the heat flux, starting at point **D**, proceeds along the same line in boiling curves, in the opposite direction, section **D**–**C**. Leap heating surface temperature decrease results from vapour bubbles spontaneous formation in the wall adjacent layer. The bubbles function as internal heat sinks, absorbing a significant amount of energy transferred to the liquid (Bilicki, 1997; Bohdal, 2001, Piasecka, 2002; Piasecka and Poniewski, 2002, 2003a,b). The shape of experimental boiling curves shown in Figs. 10 and 11 is different from the typical boiling curve (Fig. 9). The differences are clearly seen in the region of developed nucleate boiling. Such boiling curves demonstrate two-stage, "stepped" course of nucleation hysteresis in the region of developed nucleate boiling. So far similar hysteresis course, corresponding to II kind hysteresis, has manifested itself in pool boiling

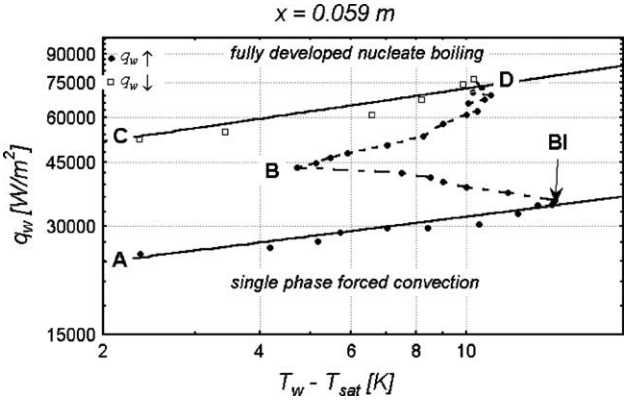

Fig. 10. Exemplary boiling curve with II kind hysteresis: $Q_V = 1.34 \times 10^{-5}$ m^3/s; $G = 502$ kg/m^2 s; $u = 0.34$ m/s; $Re = 1983$; $p_{inlet} = 179$ kPa; $\Delta T_{sub} = 32.7$ K; $q_V = 1.22 \times 10^5$–6.31×10^5 kW/m^3; $q_w = 12.4$–64.1 kW/m^2.

investigations, carried out for capillary-porous, metal and fibrous micro-surfaces, manufactured with various techniques (Poniewski et al., 2000). The above-mentioned boiling curves are characterised by smaller temperature drops, $\Delta T_{sat} = 15$–20 K (Piasecka, 2002). In both cases, for nucleate boiling, the increase in the heating surface superheating while the heat flux grows, is carried out at far lower densities of the heat flux, sections **B**–**C**, than when the heat flux diminishes, sections C–D. For decreasing densities of the heat flux, much higher values of the heat transfer coefficients are obtained. It means that nucleation centres activated while the heat flux density was growing, still remain active when the flux decreases.

The boiling curve, Fig. 11, was plotted in the system $q_w = q_w(T_w - T_l)$, not in $q_w = q_w(T_w - T_{sat})$. Such forms of boiling curves can be often found in the literature on the subject (Bohdal, 2001). Observations (Piasecka, 2002) led to the statement that at elevated pressures, $p_{inlet} > 200$ kPa, and high subcooling at the inlet, $\Delta T_{sub} > 40$ K, the local value of the saturation temperature was lower than the heating surface temperature. At the same time, the "boiling front" was observed to be correctly moving, at heat flux increase, in the direction opposite to the flow direction. That means that the temperature of the superheated wall adjacent layer was much higher than the liquid temperature in the core, and the average liquid temperature was lower than the saturation temperature. Thus, relying on the temperature difference $\Delta T_{sat} = T_w - T_{sat}$ would lead to a false conclusion that the surface is not superheated when compared with the liquid mean temperature. The instance given here refers to a vapour bubble, generated on the heating surface, which at the same time, condenses intensively in the flow core because of the low liquid temperature. Therefore, it becomes a very active heat sink, which results in the heating surface temperature drop below the local liquid saturation temperature.

8.2. Heat transfer coefficient calculation

Exemplary calculation results are presented in the form of foil temperature dependence on the distance along the channel length (Fig. 12), heat transfer coefficient dependence on the distance along the channel length, calculated according to one-dimensional model (Fig. 13) and to two-dimensional model with the application of the method of the least square (Fig. 14) and Trefftz techniques (Fig. 15). The pre-set value q_V is given in the figure Experimental parameters for the results:

- Figs. 12a, 13a, 14a and 15a: as for data presented in Fig. 6.
- Figs. 12b, 13b, 14b and 15b: as for data presented in Fig. 9.
- Figs. 12c, 13c, 14c and 15c: $Q_V = 1.0 \times 10^{-5}$ m^3/s; $G = 373$ kg/m^2 s; $u = 0.25$ m/s; $Re = 1540$; $p_{inlet} = 170$ kPa; $\Delta T_{sub} = 36.0$ K.

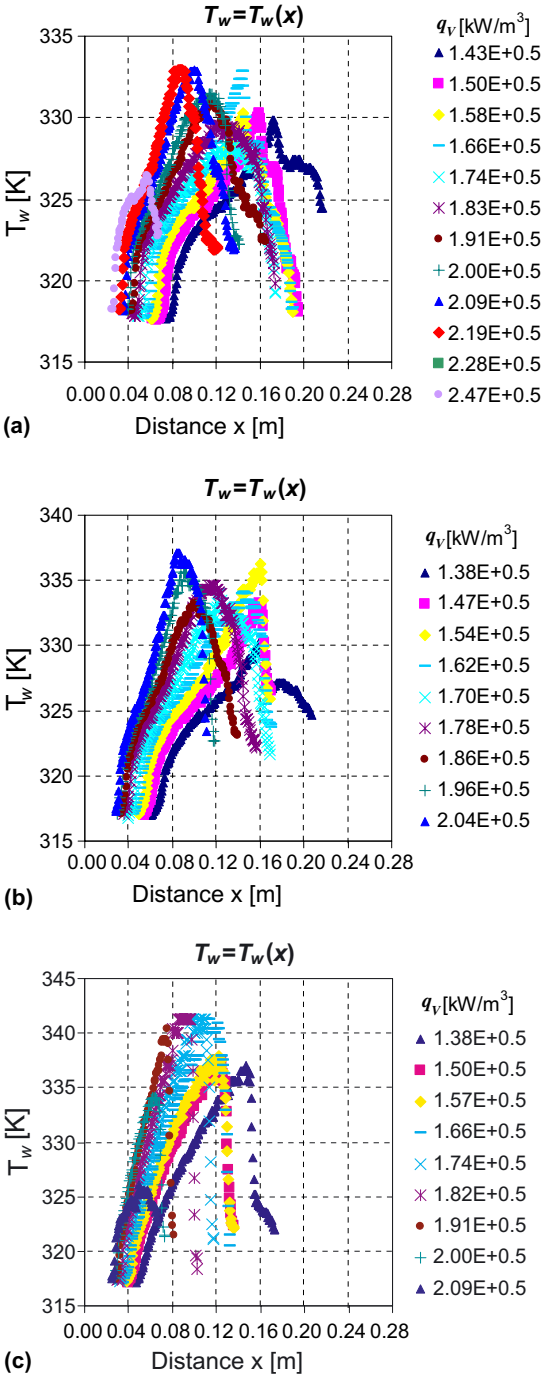

Fig. 12. Foil temperature dependence on the distance along the channel length.

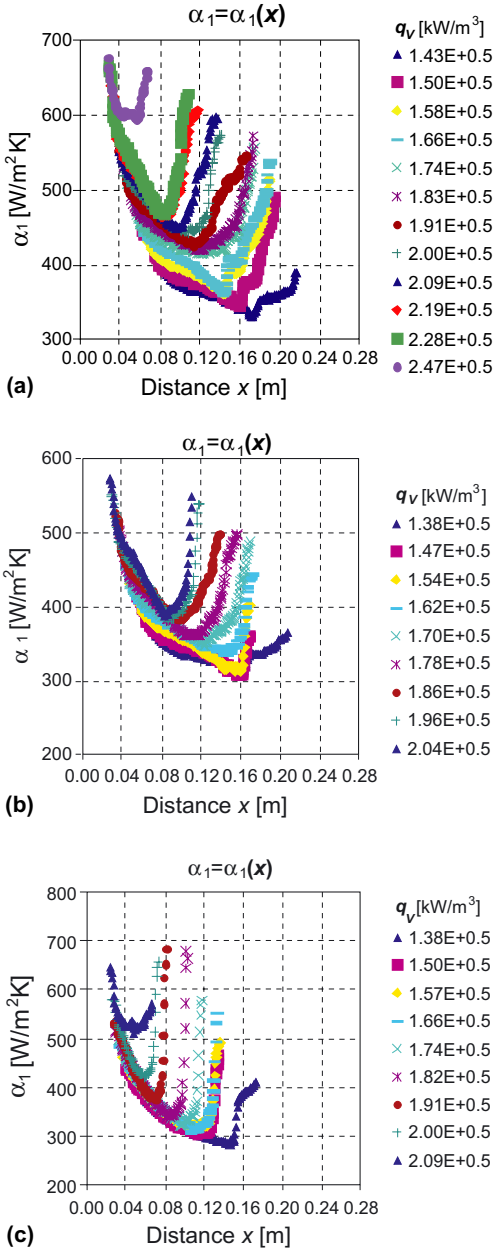

Fig. 13. Heat transfer coefficient dependence on the distance along the channel length, calculated according to one-dimensional model.

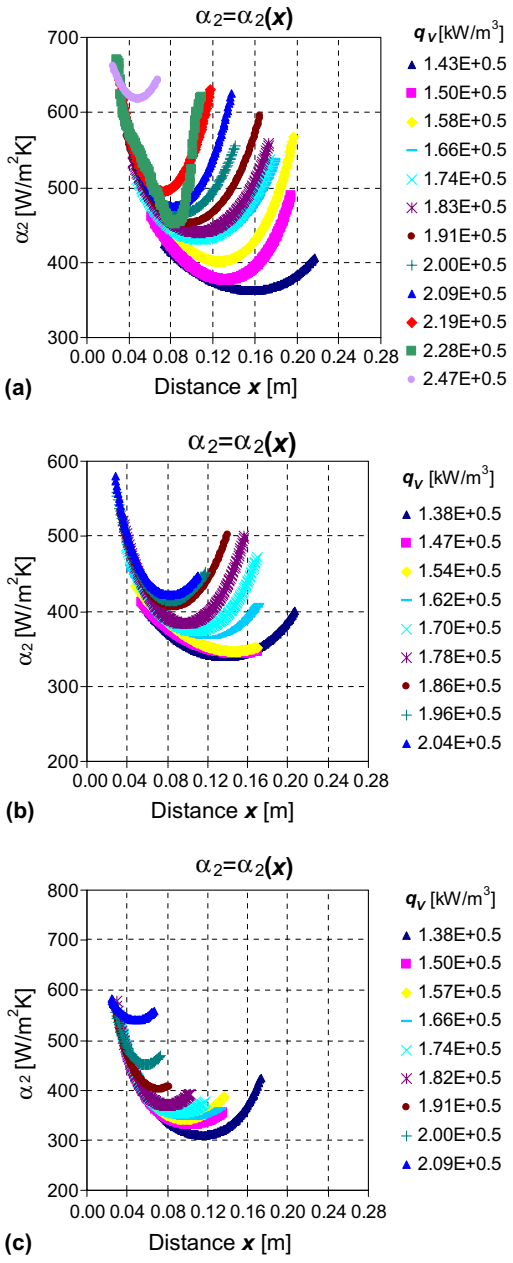

Fig. 14. Heat transfer coefficient dependence on the distance along the channel length, calculated according to two-dimensional model with the application of the least square technique.

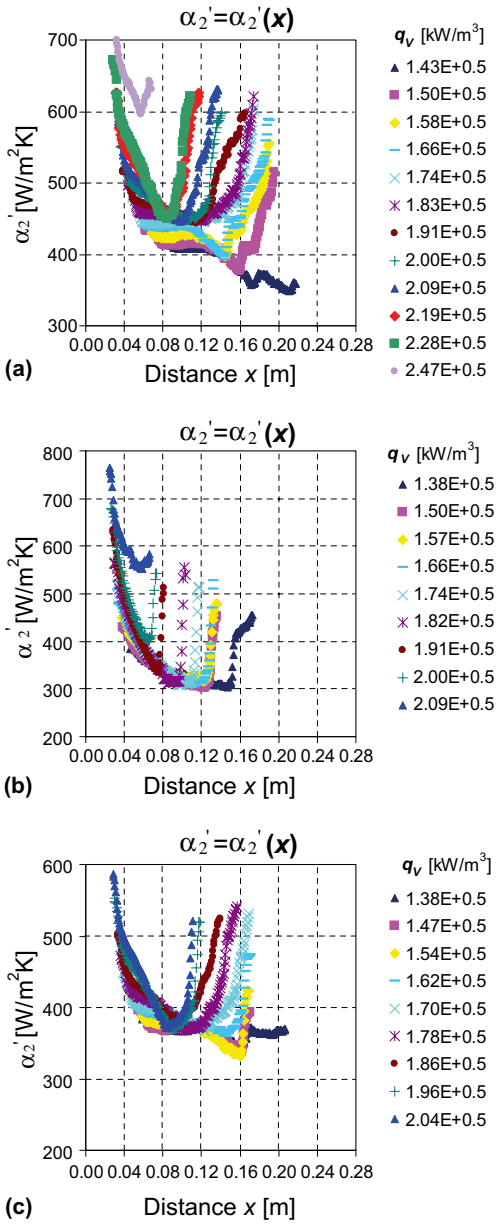

Fig. 15. Heat transfer coefficient dependence on the distance along the channel length, calculated according to two-dimensional model with the application of Trefftz technique.

9. Boiling incipience correlations

While working out the results of experimental investigations, the following similarity numbers were used (Piasecka, 2002):

- Nusselt number with heat transfer coefficient calculated from Eq. (14):

$$Nu_{\mathrm{BI}} = \frac{\alpha_{\mathrm{l,BI}} \cdot D_{\mathrm{h}}}{\lambda_{\mathrm{l}}} \tag{21}$$

- Reynolds number (Eq. (9)),
- boiling number:

$$Bo = \frac{q_{\mathrm{w,BI}}}{u} \cdot \rho_{\mathrm{l}} \cdot h_{\mathrm{lv}} \tag{22}$$

- Prandtl number:

$$Pr = \frac{\mu_{\mathrm{l}} \cdot c_{p\mathrm{l}}}{\lambda_{\mathrm{l}}} \tag{23}$$

In accordance with the requirements of dimensional analysis, the dependence for Nusselt number was written as follows (Piasecka, 2002; Piasecka and Poniewski, 2003b):

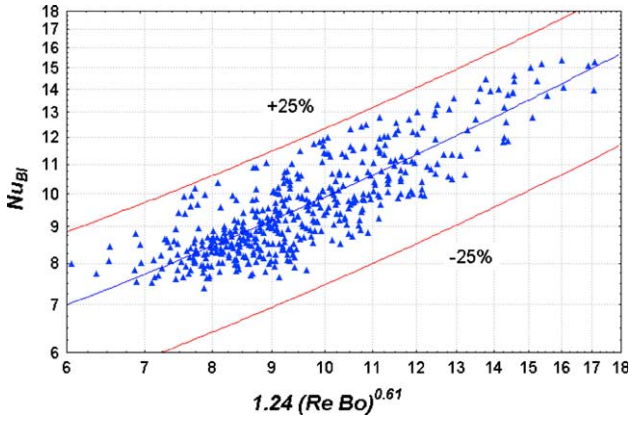

Fig. 16. Correlation for predicting R123 boiling incipience in a narrow channel, according to Eq. (26).

$$Nu_{\mathrm{BI}} = 2.39 \cdot Re^{0.63} \cdot Bo^{0.67} \cdot Pr^{-1.31} \tag{24}$$

In Eq. (24), the exponents in *Re* and *Bo* numbers are approximately of the same value, so for further considerations the product of *Re* and *Bo* numbers was assumed as one dimensionless parameter, thus arriving at the equation form:

$$Nu_{\mathrm{BI}} = 2.23 \cdot (Re \cdot Bo)^{0.64} \cdot Pr^{-1.26} \tag{25}$$

As in the range of experiments covered by the study, the values of *Pr* changed in a relatively small interval, it was removed in a subsequent equation, thus yielding:

$$Nu_{\mathrm{BI}} = 1.24 \cdot (Re \cdot Bo)^{0.61} \tag{26}$$

In order to estimate regression parameters values, 464 measurement results for R123 nucleate boiling incipience in the narrow channel were accounted for. The data were collected for point **BI**, where the constant heat flux was supplied to the heating surface. Nu_{BI} number calculated from Eq. (26)—Fig. 16, was compared with Nusselt number, determined experimentally, Eq. (21). Standard errors of calculated Nusselt number, amount to ≈0.4, whereas determination coefficients R^2, being the measure of regression line matching accuracy (in the logarithmic system)—≈0.7.

The equations analysed by the authors demonstrates congruence with over 99.6% of observable "boiling fronts", the tolerance being ±25%. These dependences refers to the following range of similarity numbers: $6.06 \leqslant Nu_{\mathrm{BI}} \leqslant 17.09$; $580 \leqslant Re \leqslant 2960$; $5.49 \leqslant Pr \leqslant 6.22$; $1.34 \times 10^{-4} \leqslant Bo \leqslant 7.00 \times 10^{-4}$.

10. Analysis of experimental data and numerical calculations

The values of local heat transfer coefficients, obtained for one- and two-dimensional models demonstrate high congruence. In general, the following regularity should be noted: heat transfer coefficient values obtained for one-dimensional model are higher than two-dimensional model ones. The differences are thought to result from simplifications assumed in one-dimensional model, which does not cover the temperature gradient in the direction perpendicular to the fluid flow. Thus, we may assume that one-dimensional model can be successfully applied to work out the results of experimental investigations concerning heat transfer in the liquid flow through a narrow vertical channel. It happens so because the local values of heat transfer coefficient are not greatly affected, provided that a very thin heater (0.1 mm) is applied. In the majority of examples, the values of the local heat transfer coefficient obtained for one-dimensional model (Fig. 13) are higher than those for the two-dimensional one, solved with the use of the least square technique (Fig. 14). On the other hand, the values of heat transfer coefficient computed with Treffz equations are generally close to, or locally higher than those resulting from one-dimensional model. The greatest divergences are observed for the highest settings q_{V} (Fig. 15a and c). The local heat transfer coefficient dependence on the distance from the inlet, determined from two-dimensional model with the use of the least square technique (Fig. 14), demonstrates polynomial character, with smoothed extremes, which leads to averaged or rounded results.

11. Conclusions

In narrow channel boiling, a considerable heat transfer enhancement took place at boiling incipience. It was observed as a sharp increase in the heat transfer coefficient. The values of the local heat transfer coefficients, obtained for one- and two-dimensional models demonstrated high congruence, which confirmed that strong simplifying assumptions were rightly made for one-dimensional model. The phenomenon of "nucleation hysteresis" was also observed, it was accompanied by a considerable heating surface temperature drop (up to 50 K). The appearance of boiling incipience was associated with the activation of some nuclei on the heated wall. It manifested itself as a sudden decrease in the wall temperature, as bubbles behaved to be acting like heat sinks. Apart from familiar shapes of boiling curves with one-step nucleation hysteresis available in the literature, a two-stepped course of the phenomenon was observed, similar to II kind hysteresis, characteristic of nucleate pool boiling on developed micro-surfaces.

The dimensionless numbers chosen to develop correlations—*Re*, *Pr* and *Bo*, yielded the best results. For the majority of the equations, almost all measurements show congruence with calculations with small tolerance ±25% which confirm a good choice for the sake of heat transfer calculations in narrow channel boiling.

Acknowledgements

The work was carried out as a part of the grant KBN 8T10B00519.

References

Adams, T.M., Abdel-Khalik, S.I., Jeter, S.M., Qureshi, Z.H., 1998. An experimental investigation of single-phase forced convection in microchannels. Int. J. Heat Mass Transfer 41, 851–857.

Adams, T.M., Dowling, M.F., Abdel-Khalik, S.I., Jeter, S.M., 1999a. Applicability of traditional turbulent single-phase forced convection correlations to non-circular microchannels. Int. J. Heat Mass Transfer 42, 4411–4415.

Adams, T.M., Ghiaasiaan, S.M., Abdel-Khalik, S.I., 1999b. Enhancement of liquid forced convection heat transfer in microchannels due to release of dissolved noncondensables. Int. J. Heat Mass Transfer 42, 3563–3573.

Ammerman, C., You, S., 1998. Enhanced convective boiling of FC-87 in small, rectangular, horizontal channels: heat transfer coefficient and CHF. ASME-HTD 357, 225–233.

Bao, Z.Y., Fletcher, D.F., Haynes, B.S., 2000a. Flow boiling heat transfer of Freon R11 and HCFC123 in narrow passages. Int. J. Heat Mass Transfer 43, 3347–3358.

Bao, Z.Y., Fletcher, D.F., Haynes, B.S., 2000b. An experimental study of gas–liquid flow in narrow conduit. Int. J. Heat Mass Transfer 43, 2313–2324.

Bar-Cohen, A., 1992. Hysteresis phenomena at the onset of nucleate boiling. Proc. Eng. Foundation Conf. Pool External Flow Boiling, Santa Barbara, USA. pp. 1–14.

Bilicki, Z., 1997. The relation between the experiment and theory for nucleate forced boiling. Proc. 4th World Conf. Experimental Heat Transfer, Fluid Mech. Thermodyn., Brussels, Belgium, vol. 2. pp. 571–578.

Bohdal, T., 2001. Development of bubbly boiling in channel Flow. Expt. Heat Transfer 4, 199–215.

Brauer, H., Mayinger, F., 1992. Onset of nucleate boiling and hysteresis effects under forced convection and pool boiling. Proc. Eng. Foundation Conf. Pool and External Flow Boiling, Santa Barbara, USA. pp. 15–36.

Celata, G.P., Cumo, M., Setaro, T., 1992. Hysteresis phenomena in subcooled flow boiling of well-wetting fluids. Expt. Heat Transfer 5, 253–275.

Chin, Y., 1997. An experimental study on flow boiling in narrow channel: from convection to nucleate boiling. Ph.D. Dissertation, University of Houston, Department of Mechanical Engineering, USA.

Chin, Y., Hollingsworth, D.K., Witte, L.C., 1998a. A study of convection in an asymmetrically heated duct using liquid crystal thermography. Proc. AIAA/ASME Thermophys. Heat Conf., Albuquerque, USA, HTD, 357-2. pp. 63–70.

Chin, Y., Hollingsworth, D.K., Witte, L.C., 1998b. Investigation of flow boiling incipience in a narrow rectangular channel using liquid crystal thermography. Proc. AIAA/ASME Thermophys. Heat Conf., Albuquerque, USA, HTD, 357-3. pp. 71–78.

Ghiaasiaan, S.M., Laker, T.S., 2001. Turbulent forced convection in microtubes. Int. J. Heat Mass Transfer 44, 2777–2782.

Hay, J.L., Hollingsworth, D.K., 1998. Calibration of micro-encapsulated liquid crystals using hue angle and a dimensionless temperature. Exp. Thermal Fluid Sci. 18, 251–257.

Hozejowski, L., Hozejowska, S., Piasecka, M., 2003. Application of harmonic polynomials as complete solutions of Laplace equation in an inverse heat conduction problem. PAMM 2 (1), 362–363.

Kuznetsov, V.V., Shamirzaev, A.S., 1999. Two-phase flow pattern and flow boiling heat transfer in non circular channel with a small gap. Proc. Int. Conf. Two-phase Flow Modelling and Experimentation, Pisa, Italy. pp. 249–253.

Lazarek, G.M., Black, S.H., 1992. Evaporative heat transfer, pressure drop and critical heat flux in a small vertical tube. Int. J. Heat Mass Transfer 25, 945–960.

McLinden, M.O., 1995. Tables and diagrams for the refrigeration industry. Thermodynamic and Physical Properties. Inernational Institute of Refrigeration, France.

Orozco, J., Hanson, C., 1992. A study of mixed convection boiling heat transfer in narrow gaps. ASME-HTD 206-2, 81–85.

Peng, X.F., Hu, H.Y., Wang, B.X., 1998. Boiling nucleation during liquid flow in microchannels. Int. J. Heat Mass Transfer 41, 101–106.

Peng, X.F., Liu, D., Lee, D.J., 2001a. Dynamic characteristics of microscale boiling. Heat Mass Transfer 37, 81–86.

Peng, X.F., Liu, D., Lee, D.J., Yan, Y., Wang, B.X., 2000. Cluster dynamics and fictitious boiling in microchannels. Int. J. Heat Mass Transfer 43, 4259–4265.

Peng, X.F., Peterson, G.P., 1996. Convective heat transfer and flow friction for water flow in microchannel structures. Int. J. Heat Mass Transfer 39, 2599–2608.

Peng, X.F., Peterson, G.P., 1995. The effect of thermofluid and geometrical parameters on convection of liquids through rectangular microchannels. Int. J. Heat Mass Transfer 38, 755–758.

Peng, X.F., Peterson, G.P., Wang, B.X., 1996. Flow boiling of binary mixtures in microchanneled plates. Int. J. Heat Mass Transfer 39, 1257–1264.

Peng, X.F., Peterson, G.P., Wang, B.X., 1995. Heat transfer characteristics of water flowing through microchannels. J. Expt. Heat Transfer 7, 265–283.

Peng, X.F., Tien, Y., Lee, D.J., 2001b. Bubble nucleation in microchannels: statistical mechanics approach. Int. J. Heat Mass Transfer 44, 2957–2964.

Peng, X.F., Wang, B.X., 1993. Forced convection and flow boiling heat transfer for liquid flowing through microchannels. Int. J. Heat Mass Transfer 36, 3421–3427.

Peng, X.F., Wang, B.X., 1994. Liquid flow and heat transfer in microchannels with/without phase change. Proc. X Int. Heat Transfer Conf., Brighton, UK, vol. 1. pp. 159–177.

Piasecka, M., 2002. Theoretical and experimental investigations into flow boiling heat transfer in a narrow channel. Ph.D. Dissertation (in Polish), the Kielce University of Technology, Department of Mechanical Engineering, Poland.

Piasecka, M., Hozejowska, S., Poniewski, M.E., 2003. Determination of local flow boiling heat transfer coefficient in narrow channel. Arch. Thermodyn. 24, 55–67.

Piasecka, M., Poniewski, M. E, 2002. Flow boiling incipience of subcooled Freon 123 in narrow rectangular channel. Proc. 3rd Int. Conf. Transport Phenomena in Multiphase Syst., Kielce, Poland. pp. 419–424.

Piasecka, M., Poniewski, M.E., 2003a. Hysteresis phenomena at the onset of subcooled nucleate flow boiling in microchannels. Proc. 1st Int. Conf. Microchannels and Minichannels, Rochester, USA, ASME, pp. 581–588.

Piasecka, M., Poniewski, M.E., 2003b. The onset of refrigerant R-123 flow boiling in a narrow vertical channel. Arch. Thermodyn. 24, 19–35.

Poniewski, M.E., Wisniewski, M.L., Wojcik, T.M., 2000. Boiling heat transfer on metal fibrous porous surfaces—experiment, model and verification. Proc. 5th Int. Conf. on Boiling Heat Transfer, Anchorage, USA, vol. 2. pp. 772–788.

Simon, T.W., 1991. Forced convection boiling on small regions. ASME/JSME Thermal Eng. Proc. 2, 259–268.

Turton, J.S., 1968. The effects of pressure and acceleration on the pool boiling of water and Arcton 11. Int. J. Heat Mass Transfer 1, 1295–1310.

Wambsganss, M.W., France, D.M., Jendrzejczyk, J.A., Tran, T.A., 1993. Boiling heat transfer in a horizontal small-diameter tube. J. Heat Transfer 115, 963–972.

Wambsganss, M.W., Jendrzejczyk, J.A., France, D.M., 1991. Two-phase flow patterns and transitions in a small, horizontal, rectangular channel. Int. J. Multiphase Flow 17, 327–342.

Wang, B.X., Peng, X.F., 1993. Boiling characteristic of subcooled liquid flowing through microchannels. Proc. VI Int. Symp. Transport Phenomena in Thermal Eng., Seoul, Korea, vol. 1. pp. 417–421.

Wang, B.X., Peng, X.F., 1994. Experimental investigation on liquid forced-convection heat transfer through microchannels. Int. J. Heat Mass Transfer 37 (Supl. 1), 73–82.

Yan, Y.Y., Lin, T.F., 1998. Evaporation heat transfer and pressure drop of refrigerant R-134a in a small pipe. Int. J. Heat Mass Transfer 41, 4183–4194.